

See discussions, stats, and author profiles for this publication at: <https://www.researchgate.net/publication/6129264>

# Surface-Enhanced Raman Signatures of Pigmentation of Cyanobacteria from within Geological Samples in a Spectroscopic-Microfluidic Flow Cell

ARTICLE *in* ANALYTICAL CHEMISTRY · OCTOBER 2007

Impact Factor: 5.64 · DOI: 10.1021/ac070994c · Source: PubMed

---

CITATIONS

35

---

READS

31

5 AUTHORS, INCLUDING:



Rab Wilson

University of Glasgow

40 PUBLICATIONS 543 CITATIONS

SEE PROFILE

# Surface-Enhanced Raman Signatures of Pigmentation of Cyanobacteria from within Geological Samples in a Spectroscopic-Microfluidic Flow Cell

Rab Wilson,<sup>†</sup> Paul Monaghan,<sup>†</sup> Stephen A. Bowden,<sup>‡</sup> John Parnell,<sup>\*,‡</sup> and Jonathan M. Cooper<sup>\*,†</sup>

Department of Electronics and Electrical Engineering, University of Glasgow, Rankine Building, Oakfield Avenue, Glasgow, G12 8LT, UK, and Department of Geology & Petroleum Geology, University of Aberdeen, Aberdeen, AB24 3UE, U.K.

A simple surface-enhanced Raman spectroscopy (SERS) microflow cell was developed to investigate distributions of scytonemin pigment within cyanobacteria from samples of rock collected from an arctic desert that contained endolithic cyanobacteria. The assay, which has future potential use in a variety of applications, including astrobiology and analysis of microorganisms in remote environments, involved studying SERS spectra of bacteria from within geological samples. By using a dispersed colloidal substrate in the microfluidic device, surface enhancement of the order  $>10^5$  was obtained for the determination of the pigment in the microorganisms when compared to the native Raman spectra. The SERS assay, which had a nM sensitivity for scytonemin, showed that the concentration of pigment was highest in samples that had experienced the highest stress environments, as a result of high doses of UV irradiation.

Raman spectroscopy has found wide application in analytical chemistry, including metabolomics, process control, and biotechnology. Despite the recent technical advances in detector sensitivity, it still suffers analytically from the relatively weak signals generated. Enhancement of the Raman effect using surface-enhanced Raman spectroscopy (SERS) results from the interaction of (bio)molecular species with metallic surfaces, particularly those of nanostructures or colloids, and can lead to greatly increased signals. In the context of this study, both scytonemin and  $\beta,\beta$ -carotene have a characteristic Raman response,<sup>1</sup> which can be enhanced through such SERS interactions.

**Significance of Pigmentation within Cyanobacteria.** Many cyanobacteria produce a number of chemical pigments when exposed to high levels of UV-A and UV-B radiation.<sup>2,3</sup> Among the

pigments produced by the cyanobacterium *Nostoc commune*, when exposed to UV-A and UV-B radiation, are scytonemin and  $\beta,\beta$ -carotene.<sup>2</sup>

Scytonemin is present within the extracellular matrix and serves as a protective sheath that can be secreted by cyanobacteria that live within high UV radiation environments.<sup>4,5</sup> Within cultures of *N. commune*, exposure to UV-B within the laboratory has been shown to be the major stimulus for the synthesis of scytonemin.<sup>2</sup>  $\beta,\beta$ -Carotene although frequently detected within cyanobacteria is not specific to them<sup>6</sup> and unlike scytonemin is found almost exclusively within the cell. However, within *N. commune*, studies have shown that levels of  $\beta,\beta$ -carotene did not increase significantly on exposure to increased UV-B radiation, although the total amounts of carotenoids did increase.<sup>2</sup> Thus, data on the relative proportions of scytonemin and  $\beta,\beta$ -carotene, present within a sample, have the potential to provide information on UV exposure and environmental stress. Current methods for achieving this typically require the removal and storage of samples, prior to sample (rock) grinding and extraction in acetone or a similar solvent. Extracts are usually analyzed by a UV–vis (200–800 nm) spectrophotometer, although HPLC may be used to provide more specific information on pigments. A screening protocol for scytonemin has also been reported using a compact mass spectrometer.<sup>7</sup> A long-term aim of our current work is to create an automated device for remote operation, exploiting the ability of a SERS-based assay to analyze biological pigments and in particular scytonemin, thereby negating the need to collect large rock samples.

**Surface-Enhanced Raman Spectroscopy.** SERS was first reported as an anomalous effect when the spectrum of pyridine on a chemically roughened silver electrode<sup>8</sup> was collected. Such roughened metal surfaces support many surface plasmons, which can be excited by laser irradiation. The curvature of the roughness on such surfaces give rise to intense electric fields generated by

\* To whom correspondence should be addressed. E-mail: j.parnell@abdn.ac.uk. Fax: +44 (0)1224 272785. E-mail: jmcooper@elec.gla.ac.uk. Tel: +44 (0)1224 273464. Fax: +44 (0)141 3306010. Tel: +44 (0)141 3304931.

<sup>†</sup> University of Glasgow.

<sup>‡</sup> University of Aberdeen.

(1) Edwards, H. G. M.; Villar, S. E. J.; Parnell, J.; Cockell, C. S.; Lee, P. *Analyst* **2005**, *130* (6), 917–923.

(2) Ehling-Schulz, M.; Bilger W.; Scherer. S. *J. Bacteriol.* **1997**, *179* (6), 1946–1950.

(3) Garcia-Pichel, F.; Sheery, N. D.; Castenholz, R. W. *Photochem. Photobiol.* **1992**, *56* (1), p. 17–23.

(4) Dillon, J. G.; Miller, S. R.; Castenholz, R. W. *Environ. Microbiol.* **2003**, *5* (6), 473–483.

(5) Dillon, J. G.; Castenholz, R. W. *Environ. Microbiol.* **2003**, *5* (6), 484–491.

(6) Palmisano, A. C.; Cronin, S. E.; Desmarais, D. J. *J. Microbiol. Methods* **1988**, *8* (4), 209–217.

(7) Hunsucker, S. W.; Tissue, B. M.; Potts, M.; Helm, R. F. *Anal. Biochem.* **2001**, *288* (2), 227–230.

(8) Fleischmann, M.; Hendra, P. J.; MaQuilla, A. *Chem. Phys. Lett.* **1974**, *26* (2), 163–166.

the excited surface plasmons.<sup>9,10</sup> Much work has been conducted on colloidal metal particles or on nanostructures,<sup>11</sup> where it has been shown that the overall enhancement is crucially dependent on the proximity of the metal particles to each other and upon their interaction with adsorbed molecules or moieties. Enhancements as large as  $10^8$  for area-averaged signals have been reported<sup>12</sup> allowing the detection of extremely low concentrations of target molecules within an assay.

**Use of a Fiber-Optic Chamber for SERS.** Recently, a relatively inexpensive optical fiber-based system for SERS has been reported in the literature.<sup>13</sup> Such a fiber-optic-based sensor system has a significant advantage over the use of conventional free space optics, in that the light exiting the fiber can occupy a small volume, giving rise to large optical field intensities. In addition, as light can be directly launched into an optical fiber, there is no requirement for a laser beam to be expanded, then collimated, in order to adequately fill an objective prior to focusing onto a sample to achieve optimum optical field intensities. The implementation of this platform together with disposable micro-channels between analyses negates the risk of carry-over between analysis. These properties, when combined with the low detection limits achievable by SERS, make such instruments suitable for the analysis of high numbers of samples, which may possess characteristically low concentrations of analyte or where only a small volume of material is available.

In this paper, we report upon a rapid SERS assay to provide quantitative information on the distribution of scytonemin within a slab of gypsum rock colonized by pigment-producing microbes. We develop a rapid method with the potential to screen for the presence of scytonemin in the field for environmental studies investigating the effects of exposure of the microbes to UV radiation.

## EXPERIMENTAL SECTION

**Optical Chamber Configuration.** A disposable microfluidic system, based upon methods adapted from ref 14, was constructed from a glass capillary tube, outer diameter  $470\ \mu\text{m}$  and inner diameter  $320\ \mu\text{m}$ , constrained within a poly(dimethylsiloxane) (PDMS) holder. The capillary tube acted as both a simple microfluidic channel and the SERS chamber. The holder for the SERS chamber incorporated an access aperture into the top of the holder for the capillary tube and side alignment channels for the input and collection optical fibers in a  $90^\circ$  configuration, a schematic of which is shown in Figure 1. The top of the holder was formed in PDMS (thickness  $\sim 5\ \text{mm}$ ) using a mold machined out of aluminum shim. The molded PDMS was bonded to a 5-mm flat piece of PDMS (pretreated with an oxygen plasma to aid bonding<sup>15</sup>). A space was left around the capillary tube to prevent the presence of background Raman bands produced by PDMS in

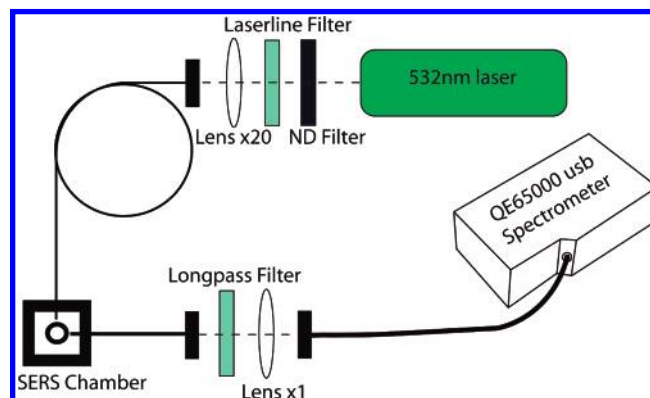


**Figure 1.** Schematic figure illustrating the configuration of the experimental setup. The output of a solid-state 532-nm laser was passed through a neutral density filter and a Thorlabs laser line filter in order to clean up the excitation radiation. The laser radiation was then end-fire launched into 2 m of optical fiber with a  $20\times$  microscope objective (Newport) to deliver  $\sim 10\ \text{mW}$  power to the SERS chamber. The scattered light was then collected via a  $650\text{-}\mu\text{m}$  core optical fiber passed through a long-pass filter and then fed into  $650\text{-}\mu\text{m}$  core patch fiber with a SMA connector connected to an Ocean Optics inc. QE65000 scientific grade spectrometer.

the sample spectra. Once assembled, no further alignment was necessary, between experimental runs.

Figure 1 shows a schematic of the setup used where the output from a 532-nm solid-state laser was passed through a neutral density filter and a Thorlabs laser line filter in order to clean up the excitation radiation. The laser radiation was then coupled to a standard communication optical fiber (Corning SMF-2e), with an  $8\text{-}\mu\text{m}$ -diameter core and  $125\text{-}\mu\text{m}$ -diameter cladding, using a  $\times 20$  objective, to provide  $10\ \text{mW}$  output at the end of the fiber. The collection optical fiber consisted of a  $650\text{-}\mu\text{m}$ -diameter core with a  $950\text{-}\mu\text{m}$  cladding. The numerical aperture of the input fiber and the collection fiber were 0.14 and 0.33, respectively. A Semrock long-pass filter ( $368\ \text{cm}^{-1}$ ) was used to reject Rayleigh scattered light and enable the detection of Stokes' scattered radiation, which was then coupled into a  $650\text{-}\mu\text{m}$  patch fiber via a  $\times 1$  magnification lens. The patch fiber was easily attached to an Ocean Optics QE65000 scientific grade USB spectrometer (spectral resolution of  $8\ \text{cm}^{-1}$ ) using a standard SMA connection. Signals were collected using a Hamamatsu back-thinned detector, cooled to  $-10\ ^\circ\text{C}$  to reduced background noise. The divergence of the radiation field of the input optical fiber was estimated using its NA, giving a probe volume of  $\sim 75\ \text{pL}$  within the microfluidic channel.

**Materials.** The chemicals used in this study, including silver nitrate, hydroxylamine hydrochloride, sodium hydroxide, dimethyl sulfoxide (DMSO), methanol, and rhodamine-6G, were obtained from Sigma-Aldrich. Scytonemin, as a standard calibrant, was purchased from Calbiochem, a subsidiary of Merck.

**Colloid Preparation and Analysis.** Silver colloid was prepared as previously described,<sup>16</sup> in which  $10\ \text{mL}$  of silver nitrate solution ( $10^{-2}\ \text{M}$ ) was added gradually to a continuously stirred  $90\text{-mL}$  solution of hydroxylamine hydrochloride ( $1.67 \times 10^{-3}\ \text{M}$ ) and sodium hydroxide ( $3.33 \times 10^{-3}\ \text{M}$ ). All reagents were prepared immediately prior to colloid preparation (otherwise an unstable colloid was produced, providing little or no surface-

(9) Moskovits, M. J. *Raman Spectrosc.* **2005**, *36* (6–7), 485–496.

(10) Poliakov, E. Y.; et al. *Opt. Lett.* **1996**, *21* (20), 1628–1630.

(11) Baia, M.; Baia, L.; Astilean, S. *Chem. Phys. Lett.* **2005**, *404* (1–3), 3–8.

(12) Haynes, C. L.; Van Duyne, R. P. *J. Phys. Chem. B*, **2003**, *107* (30), 7426–7433.

(13) Young, M. A.; Stuart, D. A.; Lyandres, O.; Glucksberg, M. R.; Van Duyne, R. P. *Can. J. Chem.: Rev. Can. Chim.* **2004**, *82* (10), 1435–1441.

(14) Berthod, A.; Laserna, J. J.; Winefordner, J. D. *Appl. Spectrosc.* **1987**, *41* (7), 1137–1141.

(15) Duffy, D. C.; McDonald, J. C.; Schueller, O. J. A.; Whitesides, G. M. *Anal. Chem.* **1998**, *70* (23), 4974–4984.

(16) Leopold, N.; Lendl, B. *J. Phys. Chem. B* **2003**, *107* (24), 5723–5727.

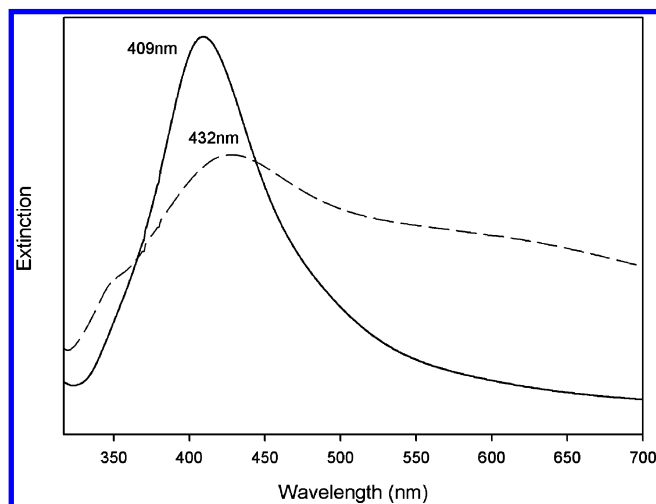


**Figure 2.** Extinction spectra of hydroxylamine-reduced silver colloids where 10 mL of silver nitrate was added dropwise (solid line) or rapidly (dashed line) to 90 mL of hydroxylamine/sodium hydroxide. An extinction maximum at 409 nm is consistent with that of Leopold and Lendl,<sup>16</sup> implying an average size of 23 nm for the silver nanoparticles.

enhanced Raman scattering). UV–vis absorbance spectra of the colloids were collected on a Hitachi U2000 spectrophotometer. Figure 2 compares the quality of the colloid when produced either by gradual (dropwise) addition or by bulk mixing. Colloidal silver was stored in a dark environment at a constant temperature of 4 °C.

**Stock Solution Preparation.** Scytonemin standards were used without any further processing to estimate the analytical sensitivity of detection and to confirm Raman band assignments during SERS on field samples. For standard preparation, a 1-mg standard of the pigment was dissolved in DMSO to provide a stock solution of 100  $\mu$ M concentration from which a series of standard dilutions were made in deionized water. DMSO is miscible with water and thus enables the use of various water-insoluble compounds with aqueous colloids (assuming that they do not precipitate).

**Analysis and Processing of Microbial-Colonized Gypsum.** Sampling was optimized in order to process multiple samples in large batches, as quickly as possible. The sample material analyzed in the study comprised small blocks of transparent gypsum that were colonized by cyanobacteria (*Gloeocapsa* and *Nostoc*), which grow along natural fissures within the rock.<sup>17,18</sup> Colonies of cyanobacteria are common within arctic environments where they can be important primary producers.<sup>19</sup> Coloration varies throughout the samples. Samples collected from the edge of the gypsum (Figure 3) possess colonies of cyanobacteria that are black or brown, while samples collected from deeper within the fissure have colonies that are pink or green. Two small samples of transparent gypsum,  $\sim 1$  cm<sup>2</sup> and weighing  $\sim 5$  g, colonized by microbes were mechanically homogenized to a fine powder. The material was transferred to a 25-mL beaker to which 2 mL of

methanol was added in order to lyse cellular material and increase the amounts of free pigment. Beakers containing the methanol and sample were placed into an ultrasonic bath for 15 min to speed up cell lysis. After sonification, the methanol was evaporated off and the sample resuspended in 1 mL of DMSO. Microliter quantities of the gypsum extract were added to the colloid without filtering (it was noted that the contribution due to light scattering was minimal). A 30- $\mu$ L sample of 1 M sodium hydroxide was added to the mixture to aggregate the silver colloid prior to a SERS measurement. All measurements were made in triplicate.

**Curve Fitting of Data.** Curve-fitting analysis of the collected Raman spectra was carried out using PeakFit software published by AISN Software Inc. All the peaks analyzed were fitted using symmetric Gaussian functions having a profile with constant width. Each spectrum was smoothed by 1% using the Savitzky–Golay algorithm prior to fitting. A methodology given by ref 20 was used to obtain the best fit where a minimal number of bands were initially used and subsequently increased until no further improvement in the fit was observed.

## RESULTS AND DISCUSSION

**Raman Spectra of Standards and Limits of Detection.** The Raman spectrum for the initial 1 mM solution of scytonemin in DMSO is shown in Figure 4a, taken without the aid of silver colloid. No Raman peaks could be distinguished due to autofluorescence from the sample. A 10- $\mu$ L quantity of the 100  $\mu$ M standard was then added to colloidal silver to provide a 1  $\mu$ M final concentration for scytonemin. The spectra from this solution (Figure 4a) showed a significant improvement in the signal, and spectral features of scytonemin could be clearly observed.

SERS spectra were collected for various standard dilutions of the 100  $\mu$ M stock solution of scytonemin in DMSO, to produce a calibration curve for the detection of the unique cyanobacterial pigment scytonemin (Figure 4b). For a concentration of 2 nM, the signal obtained was  $>3\sigma$  above the mean of the background noise, and this figure of merit was thus used to define the limit of the detection. The difference between the concentration of the initial stock solution and the limit of detection was used as an estimate for the enhancement factor provided by the silver colloid,<sup>16</sup> which in this case was of the order  $10^5$ . Such enhancements compare favorably to other published data,<sup>9,12,13,21</sup> demonstrating the much improved sensitivity provided by SERS compared to normal Raman spectroscopy.

**Analysis of Samples of Gypsum Colonized by Cyanobacteria.** The SERS assay required a small amount of sample material (125 mg), demonstrating the applicability of the technique to the analysis of geological samples from remote environments. Figure 5 shows the strong SERS response, observed for a 25- $\mu$ L fraction of a 200- $\mu$ L extract from the black colonies.

The smallest sample size of pink colonized gypsum that yielded a sufficiently high signal/noise spectra was approximately double that of the black colonies (50  $\mu$ L from 200  $\mu$ L of resuspended extract), Figure 5. Again the presence of scytonemin can be clearly seen. The spectra obtained from both the black and pink colonies are similar except the pink samples always exhibit a lower

(17) Cockell, C. S.; Lee, P.; Osinski, G.; Horneck, G.; Broady, P. *Meteorit. Planet. Sci.* **2002**, *37* (10), 1287–1298.

(18) Parnell, J.; Lee, P.; Cockell, C. S.; Osinski, G. R. *Int. J. Astrobiol.* **2004**, *3* (03), 247–256.

(19) Quesada, A. V. W. F.; Lean, D. R. S. *FEMS Microbiol. Ecol.* **1999**, *28* (4), 315–323.

(20) Mysen, B. O.; Finger, L. W.; Virgo, D.; Seifert, F. A. *Am. Mineral.* **1982**, *67* (7–8), 686–695.

(21) Zou, X. Q.; Dong, S. J. *J. Phys. Chem. B* **2006**, *110* (43), 21545–21550.



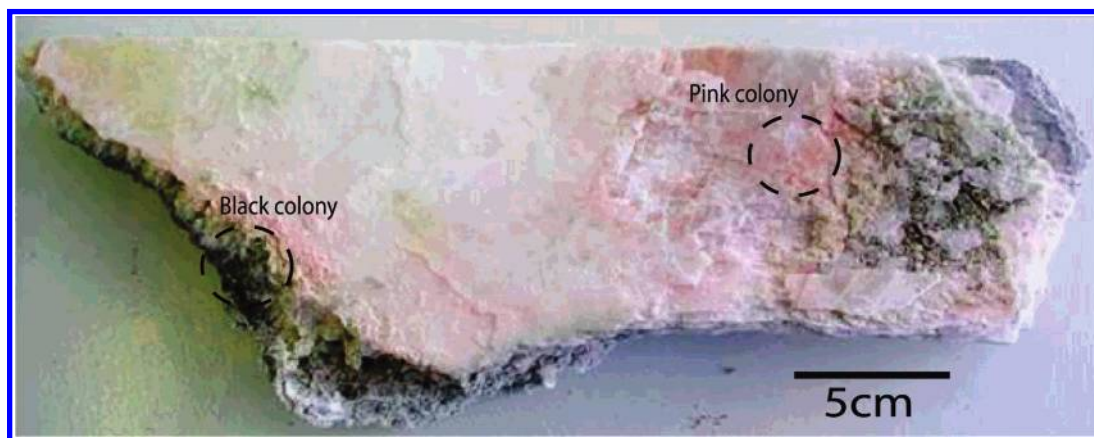


**Figure 3.** Sample of gypsum collected from the Haughton impact crater, in the Canadian arctic. There are a number of microbial colonies inhabiting the translucent rock as indicated by their variation in pigmentation. Indicated is the sampled black colony living in the outer crust of the rock and the sampled pink colony living in the interior of the gypsum.

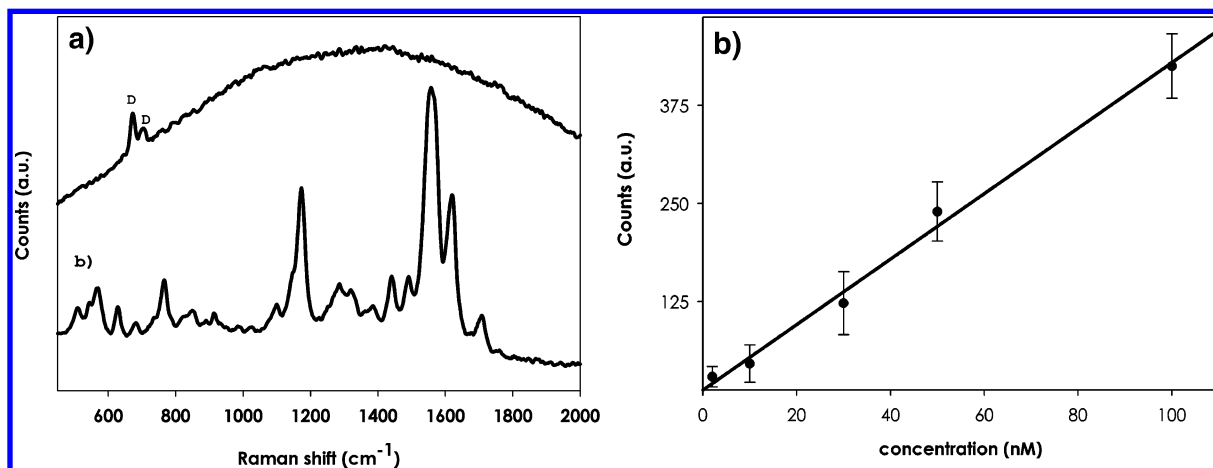


**Figure 4.** (a) Raman spectrum of 1000  $\mu\text{M}$  concentration of scytonemin solvated in DMSO. The spectrum was taken with 10 mW and an integration time of 4 s, and results were averaged for three spectra. None of the characteristic fingerprint peaks for scytonemin were observed; only peaks associated with DMSO were recorded. A 10- $\mu\text{L}$  sample of the 100  $\mu\text{M}$  scytonemin solution was added to silver colloid to provide a concentration of 1  $\mu\text{M}$ . The Raman spectrum (b) of the 1  $\mu\text{M}$  solution taken under the same conditions showed bands that are associated with scytonemin. This figure illustrates the significant enhancement that can be obtained with SERS. It should also be noted that peaks associated with DMSO are absent in (b) as the DMSO was diluted, together with the scytonemin, 100-fold. b: Calibration curve for scytonemin (1176  $\text{cm}^{-1}$  peak). Scytonemin was added directly to the colloid and then 30  $\mu\text{L}$  of sodium hydroxide 1 M solution was added to aggregate the colloid. The spectra for each were taken using 532 nm, 10 mW laser irradiation using a 4 s integration time with data averaged over three experiments for each sample. The calibration curve is linear response ( $r^2 = 0.961$ ) to 10 nM concentration, although at 2 nM concentrations we observed signals three times that of the standard deviation of the background noise.

magnitude of characteristic Raman responses, indicative of a lower concentration of scytonemin. Other differences can also be observed: one of the fingerprint Raman bands at 1323  $\text{cm}^{-1}$  (previously reported<sup>22</sup> as assigned the C=N bond in the indole ring structure found in scytonemin) is not well developed but manifests as a broad spectral feature in the extracts of colonized gypsum. This “peak” is apparent at higher concentrations, as can be seen in the spectrum of the 1  $\mu\text{M}$  scytonemin in silver colloid shown in Figure 4a.

While the spectral characteristics of scytonemin can clearly be identified within the SERS spectra presented, other spectral characteristics suggestive of carotenoids appear within the extracts of the pink and black endolithic microbial colonies (Figure 5). In order to resolve the difference in pigmentation between the black

and pink colonies, their spectra were analyzed by curve fitting of the composite peak situated at 1176  $\text{cm}^{-1}$  (Figure 6) using methods described by ref 20. Further, using Raman spectra first published by Howell et al.,<sup>22</sup> bands situated at 1162 and 1172  $\text{cm}^{-1}$  were used to deconvolve this 1176  $\text{cm}^{-1}$  composite peak.

It was found that four bands, situated at 1139, 1144, 1156, and 1182  $\text{cm}^{-1}$  could be used to accurately fit the experimentally observed 1176  $\text{cm}^{-1}$  peak for both colonies. The fitted band situated at 1156  $\text{cm}^{-1}$  can readily be assigned to the  $\nu 1$  band of  $\beta, \beta$ -carotene. There are other carotenoid pigments such as zeaxanthin, canthaxanthin, and enchinone that possess long conjugated chains that are known to be present in cyanobacteria;<sup>6</sup>

(22) Edwards, H. G. M.; Garcia-Pichel, F.; Newton, E. M.; Wynn-Williams, D. D. *Spectrochim. Acta, Part A: Mol. Biomol. Spectrosc.* **2000**, *56* (1), 193–200.

(23) Withnall, R.; Chowdhry, B. Z.; Silver, J.; Edwards, H. G. M.; de Oliveira, L. F. C. *Spectrochim. Acta, Part A: Mol. Biomol. Spectrosc.* **2003**, *59* (10), 2207–2212.

(24) Merlin, J. C. *Pure Appl. Chem.* **1985**, *57* (5), 785–792.

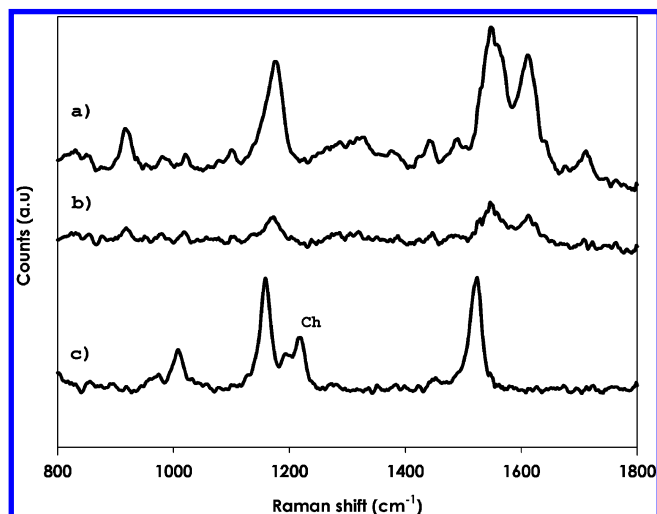


**Figure 5.** SERS spectra of (a) a 50  $\mu\text{L}$  extraction from a black colony, compared with (b) a 50  $\mu\text{L}$  extraction from a pink colony. The power used for both spectra was 10 mW with an integration 4 s averaged over three consecutive scans. For reference, these are compared to (c), which shows Raman spectra taken on current setup of 7  $\mu\text{M}$   $\beta,\beta$ -carotene in chloroform, where the three strongest bands are clearly visible alongside a chloroform peak (ch). The power used was 10 mW with an integration time of 10 s averaged over 3 scans. It is clear from the data that scytonemin was present in the black colony in significantly larger amounts than in the pink colony. There appears to be an overlap between the  $\nu_1$  and  $\nu_2$  bands of  $\beta,\beta$ -carotene and that of microbially derived spectra.

such compounds also display  $\nu_1$  and  $\nu_2$  Raman spectral characteristics very similar to  $\beta,\beta$ -carotene.<sup>23,24</sup>

In addition, it is possible that processing of the material can cause the formation of cis-isomers, which can lead to the production of multiple Raman bands in the range 1100–1300  $\text{cm}^{-1}$ .<sup>24</sup> It is therefore possible that the fitted band positioned at 1144  $\text{cm}^{-1}$  may be attributed to such compounds. The fitted band positioned at 1139  $\text{cm}^{-1}$  may be assigned to C–H stretching while the weak band positioned at 1203  $\text{cm}^{-1}$  may be assigned to C–H bending.

Surface-induced effects may explain the observation of the band situated at 1182  $\text{cm}^{-1}$  (within the 1176  $\text{cm}^{-1}$  composite peak). HPLC would be required to obtain a full inventory of biomolecules present in the extract in order to confidently assign these bands, which will be the subject of a further study.

Having inferred the presence  $\beta,\beta$ -carotene from the band 1156  $\text{cm}^{-1}$  presented in the fitted data, information concerning the ratio of  $\beta,\beta$ -carotene to scytonemin may be calculated using the strong 1172  $\text{cm}^{-1}$  band reported by Howell et al.<sup>22</sup> The ratio of the areas of the fitted bands (Figure 6) for the 1156 and 1172  $\text{cm}^{-1}$  bands contained in the 1176  $\text{cm}^{-1}$  composite peak indicated a difference in the concentrations of  $\beta,\beta$ -carotene with respect to scytonemin for the black (0.33) and the pink (0.55), implying an environmental influence on the ratio of the two pigments.

Lakatos et al.<sup>25</sup> observed little dependence of the carotenoid content in cyanobacteria with UV exposure, although, they did see a trend in the relative amounts of  $\beta,\beta$ -carotene, echinenone, and canthaxanthin, where the quantity of canthaxanthin was found to increase relative to  $\beta,\beta$ -carotene and echinenone with the extent

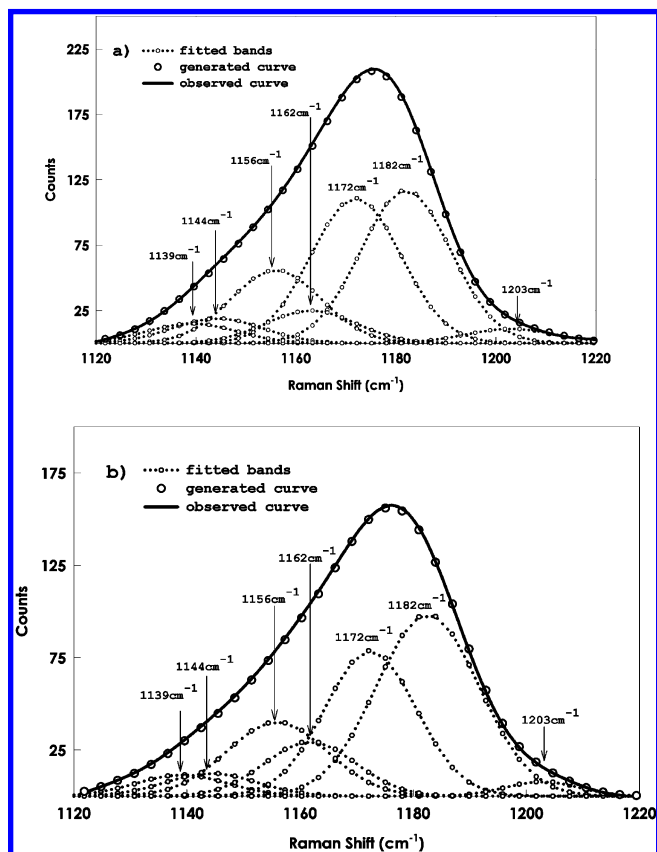


**Figure 6.** Expanded plots of the composite 1176- $\text{cm}^{-1}$  peak. Shown where fitted band contributions and generated curves are plotted in (a) for the BLK-1 sample taken from the black colony and in (b) for the Pink-1 sample taken from the pink colony. The broadness of the peak suggests contributions from biomolecules other than scytonemin. A fitted band situated at 1156  $\text{cm}^{-1}$  present in both spectra is suggestive of  $\beta,\beta$ -carotene.

of sunlight exposure. The molecular structure of canthaxanthin is very similar to  $\beta,\beta$ -carotene (with the exception of a carbonyl group in each cyclohexane ring), and it is not possible to distinguish each carotenoid, from these data. Therefore, the ratio values for both microbial communities would be consistent with the interpretation that the pink colonies contained a lower quantity of the UV filter scytonemin than the black colonies. Other workers have previously observed pink or green coloration as opposed to black or brown coloration in endolithic communities collected from deeper within microbial crusts.<sup>17</sup> Thus, our measurements add weight to support the hypothesis that cyanobacteria produce scytonemin into the extracellular matrix, as a protective molecular filter when their exposure to UV radiation is higher.

## CONCLUSION

We have shown that SERS can be used to detect scytonemin, the sheath pigment unique to cyanobacteria, at nM concentrations, using a small, light, and low-cost system. The relatively low spectral resolution of the spectrometer used in this study represents a common constraint of all current field-deployable spectrometers. In the longer term, this SERS assay may benefit from the introduction of a preparative chromatographic and liquid–liquid or solid-phase extraction step to separate mixtures of pigments and present the compounds individually for SERS analysis. Although implementing such processing in the field

(25) Lakatos, M.; Bilger, W.; Budel, B. *Eur. J. Phycol.* **2001**, *36* (4), 367–375.

would involve complex integration, we are currently exploring microfluidics as a viable technology to achieve this.<sup>26</sup>

## ACKNOWLEDGMENT

This work was supported by EPSRC grant GR/S47267/01. Samples of microbe bearing gypsum were collected by S.A.B.

---

(26) Bowden, S. A.; Monaghan, P. B.; Wilson, R.; Parnell, J.; Cooper, J. M. *Lab Chip* **2006**, 6 (6), 740–743.

while conducting field work at the NASA-CSA Haughton-Mars Project on Devon Island. We are grateful to the Polar Continental Shelf Project (Natural Resources Canada), the Nunavut Research Institute, and the Communities of Grise Fiord and Resolute Bay for their support.

Received for review May 16, 2007. Accepted June 29, 2007.

AC070994C